

Flow Characteristics around a Valve Plate Installed in a Duct *
(2nd Report, Swing Type Valve Plate Installed in a Chamber)

By Junichi KUROKAWA**, Akira TAKAGI***,
 Toshiyuki UCHIDA+ and Takashi KUSA++

The steady flow characteristics around a swing-type valve plate installed in a rectangular duct are studied theoretically and experimentally in order to determine the fluid force acting on a swing-type check valve and the side-gap-leakage effects.

The results show that the side-gap leakage has dominant influence upon the fluid force characteristics, which can be well predicted by a small modification of the conventional two-dimensional potential flow theory. For the case of a large side gap, the pressure over the valve plate becomes nearly uniform and is equal to the upstream one. And that the fluid force is expressed as a function of only the velocity ratio of the jet to the upstream, if the side-gap-leakage is less than the mainflow volume. It is pointed out that the separation zone at the back of a valve plate is recovered very rapidly due to momentum transfer effects of side-gap-leakage, and that the outlet flow from a valve plate is not contracted with its width nearly equal to the valve opening one. The experimental formulae of moment coefficient are also presented.

Key Words: Fluid Machine Element, Swing Check Valve, Duct Flow, Leakage, Side Gap, Back Pressure, Moment Coefficient

1. Introduction

In the former report⁽¹⁾ the flow characteristics around a swing-type valve plate installed at the exit of a rectangular duct were studied experimentally in order to determine flap valve performances fundamentally, and it was shown that lateral leakage from both plate side-gaps has dominant influence upon the valve performances and experimental formulae of fluid force were presented.

In high head pump pipe-lines a swing type check valve is usually used to prevent a reverse flow at the stop of pumping. In this type of a valve the downstream is restricted by a pipe wall and accordingly the flow pattern of a valve outlet flow is considered much different from that of a flap valve, and side-gap-leakage might also have large influence on the check valve performances, as suggested by the results of a flap valve.

As is already surveyed in the former report, studies about such flow characteristics are very few⁽²⁾⁽³⁾ and it is still difficult to predict the fluid force of a swing-type check valve and side-gap-leakage

effects, though there are many about water hammer phenomena of a pipe-line system with a swing type check valve as a component.

The present study is aimed to determine the steady flow characteristics around a valve plate installed in a duct, the fluid force and the side-gap-leakage effects theoretically and experimentally in order to have fundamental knowledge on swing type check valve performances.

2. Theory

A two-dimensional flow model around a swing-type valve plate installed in a duct is shown in Fig.1. Birkhoff et al.⁽⁴⁾ have analyzed this flow using potential flow theory with a Hodograph-method. But according to the measured results shown later, the three-dimensional leakage from the valve side-gaps has large influence upon the flow characteristics, and especially for the case of a small valve opening angle it has dominant influence. It is in general very difficult to predict the three-dimensional effects of the flow by two-dimensional theory. Therefore, an approximate method is proposed here to predict the side-gap leakage effects by modifying the conventional two-dimensional potential flow theory.

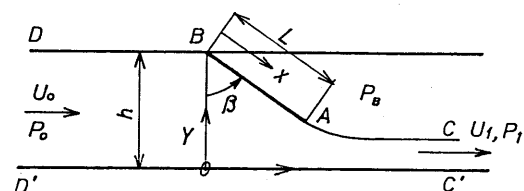


Fig. 1 Two-dimensional flow model.

* Received 19th December, 1983
 ** Associate Professor, Yokohama National University, 156 Tokiwadai, Hodogaya, Yokohama, 240 Japan.
 *** Graduate Student, Yokohama National University.
 + Engineer, Torei Co. Ltd., 9-1 Ooecho, Minato-ku, Nagoya, 455 Japan.
 ++ Engineer, Toshiba Co. Ltd., 1 Toshihba-cho, Fuchu, Tokyo, 183 Japan.

For the sake of simplicity of the analysis, velocities are normalized by the infinite downstream velocity U_1 , that is $U_1=1$, and the upstream one is V , the flow volume is π per unit time and unit channel width as shown in Fig.2. The complex velocity $u+iv$ (u and v are the horizontal and the vertical velocity components, respectively) on the boundary streamlines DBAC and $D'C'$ is mapped onto the fan-shape in the Hodograph plane(ζ -pl) in Fig.3. Using the Schwartz-Christoffel transformation it is again mapped onto the straight line and the flow field is mapped onto the half-infinite plane, and the complex potential $W(\zeta)$ in ζ -plane is determined as follows by placing a source and a sink at the corresponding points to the infinite upstream D, D' and the infinite downstream C, C' .

$$W(\zeta) = \ln(\zeta^n - V^n) - 2\ln(\zeta^n - 1) + \ln(\zeta^n - 1/V^n) \dots (1)$$

where $\pi/n = \pi/2 - \beta$. The value of the valve plate length L is also determined by the given configuration of a duct assembly as follows using a radius R along BA in ζ -pl.

$$\pi L/hV = \int_0^1 \{1/(R^n + V^n) + V^n/(R^n V^{n+1}) - 2/(R^{n+1})\} nR^{n-2} dR \dots (2)$$

If it were not for lateral leakage, all the flow volume would leave in the downstream direction. Then the existence of lateral leakage from both side-gaps of a plate leads to reducing the downstream velocity U_1 , or increasing the upstream velocity V to $V+\Delta V$ for the constant downstream velocity $U_1=1$. Considering this in the Hodograph-plane, the ordinates of the infinite points D and D' are shifted to E . Thus, the complex potential $W(\zeta)$ is obtained only by replacing V by $V + \Delta V$ in Eqs.(1) and (2) when there is lateral leakage.

Considering this again in the physical plane, the above-described procedure changes the duct dimension L/h as shown in Fig. 4(b), as an example, because the equation of continuity requires that all the inflowing volume be strictly equal to the outflowing volume for an incompressible fluid. That is to say, this procedure approximates the flow field such that the duct height h is enlarged to accommodate the leakage volume for the same upstream velocity V and the same plate length L .

The leakage volume $\pi \Delta V/V$ from both side gaps is estimated approximately as follows using the pressure difference of the plate $P-P_B = \rho(1-c^2)/2$ for the case of no leakage, the side clearance t and the plate lateral width B :

$$\Delta V = (2Lt/hB) \int_0^1 \sqrt{1-c^2} dS \dots (3)$$

where c is the absolute velocity along the valve plate and $S=x/L$.

As an example, the stream lines are calculated for the case of the valve opening angle $\beta = 40^\circ$ and the gap ratio $2t/B = 0.11$, and are compared in Fig.4(a) and (b) with those of no leakage($t=0$). It is here recognized that the flow volume of $\psi/U_0h =$

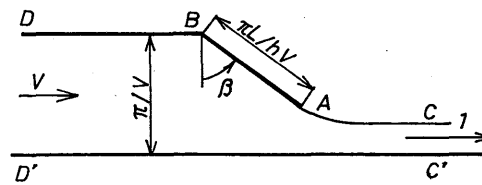


Fig. 2 Flow model used in analysis. (Physical plane)

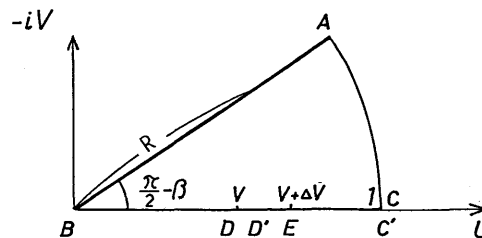
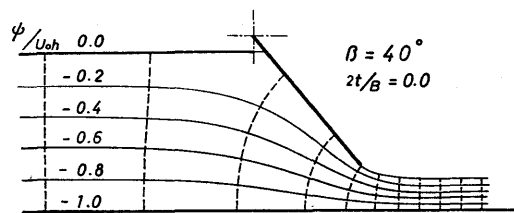
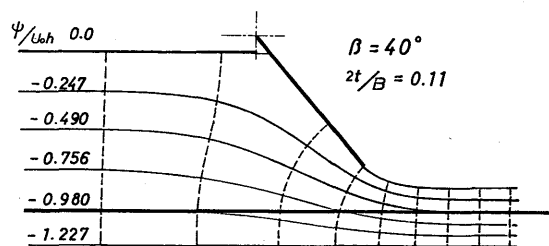


Fig. 3 ζ - plane(Hodograph plane).



(a) In the case of no leakage ($t=0$) (Two-dimensional theory).



(b) In the case of side-gap leakage. Fig. 4 Comparison of stream lines with and without side-gap leakage.

$-0.49 \sim -1.0$ (ψ is a stream function) goes out from the lower wall and this volume corresponds to the leakage volume from the side gaps. That is, about a half the inflowing volume becomes side gap leakage, which results in reduction of the pressure drop along a valve plate, the jet velocity and the back pressure.

3. Experimental Apparatus and Procedures

Experimental apparatus is shown in Fig.5. A rectangular duct of $h=300$ mm in height, $B'=180$ mm in width and $L'=2270$ mm in length is installed at the exit of a wind tunnel, and a valve plate of $L=322$ mm in length and $B=198$ mm in width is set in the valve chamber with its upper end rotatably supported. The side gap t can be varied

by inserting a spacer.

Velocity distributions in the upstream and the downstream sections, pressure distributions on the valve plate and the side wall and moment around the valve axis were measured for various valve opening angles β between 10° and 80° and various side gaps t between 1mm and 21mm with a constant upstream velocity U_0 . The measurements were performed in the range of the Reynolds numbers $1 \times 10^5 < Re < 3 \times 10^5$, where Re is defined as $U_0 h / \nu$.

4. Measured Results and Comparison with Theory

4.1 Outlet flow characteristics from a valve plate

At the exit of a valve plate the main-flow becomes a jet and a separation zone is formed just behind the valve plate. Figure 6 shows the variation of a velocity distribution toward the downstream in the case of a valve opening angle $\beta = 50.5^\circ$ (Fig. 6(a)) and 32° (Fig. 6(b)). It is seen that both the recovery of the separation zone and the reduction of jet velocity have somewhat different tendencies in these two cases. In Fig. 6(a) the recovery of the separation zone is very slow and the velocity reduction in jet region is very small, but in Fig. 6(b) the recovery of the separation zone is rapid and the velocity reduction in jet is very large. Though not shown in the figure, the recovery is more rapid for the case of $\beta = 21.5^\circ$, and the velocity distribution in the duct section is almost uniform at $x/h = 1.43$. Thus, the outlet flow has two different behaviours at larger and smaller plate angles β than 40° in both the reduction of jet region and the recovery of the separation zone.

As for the reduction of jet velocity, it is considered to be dependent upon the existence of the potential core region in jet region, where the velocity distribution is flat. In the case of $\beta = 50.5^\circ$ a potential core is maintained till the downstream, but in the case of $\beta = 32^\circ$ it does not exist any more in the jet region. To make it clearer, the variation of jet width h_j or h_j' (defined in the figure) is shown in Fig. 7 for the variation of β . The value h_j corresponds to the potential core width and is seen to increase largely in the range $\beta > 40^\circ$ and little in the range $\beta < 40^\circ$ with an increase in β , and is also seen to change little with the change of a side-gap clearance. In Fig. 7 is also shown the valve opening width h_0 by a chain-dotted line. It is seen that the jet width h_j' is nearly equal to h_0 for the range of $\beta > 40^\circ$, which means that the outlet jet flow is not contracted and its width is nearly equal to the valve opening one. In the former report⁽¹⁾ it is pointed out that the outlet flow from a flap valve plate is contracted to about 60% of the valve opening width, which is similar to the separated discontinuous flow from an orifice. Present results have revealed that the outlet flow from a swing-type check valve plate has similar characteristics to a nozzle outlet

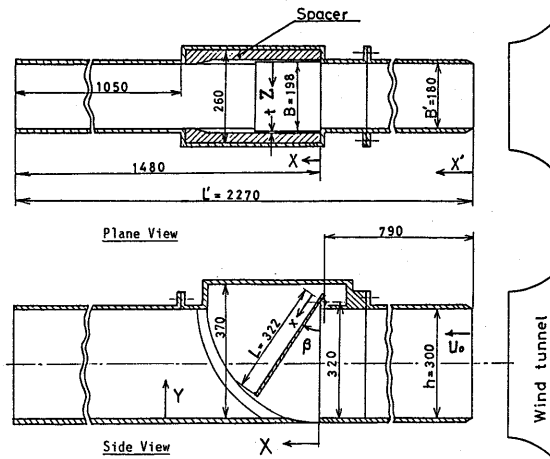
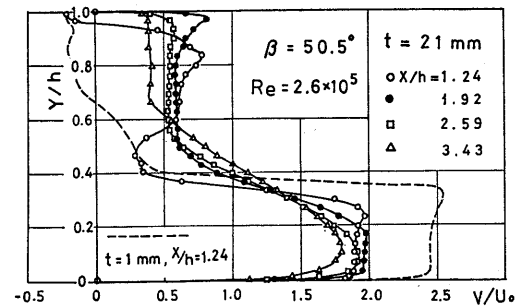
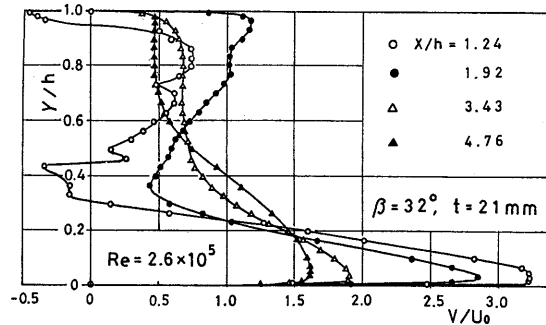


Fig. 5 Experimental apparatus. (Dimensions; mm)



(a) In the case of $\beta = 50.5^\circ$.



(b) In the case of $\beta = 32^\circ$.

Fig. 6 Velocity distribution in the section behind a valve plate ($Z/B' = 0.5$).

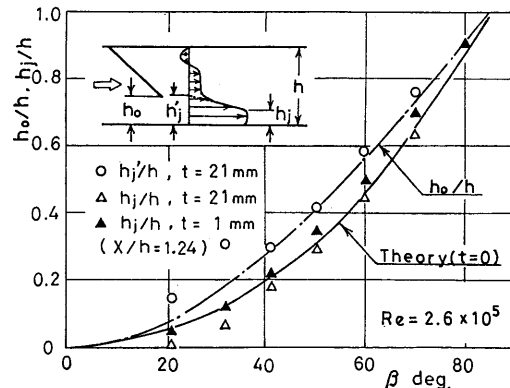
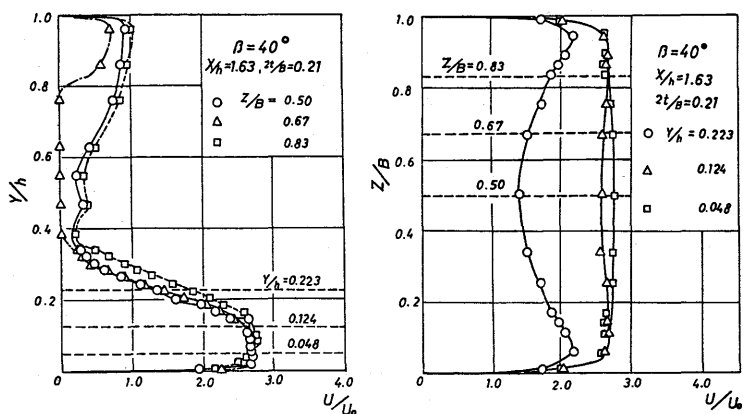


Fig. 7 Variation of jet width and valve opening width for variation of β .



(a) In horizontal plane. (b) In vertical plane.
Fig. 8 Velocity distribution behind a valve plate.

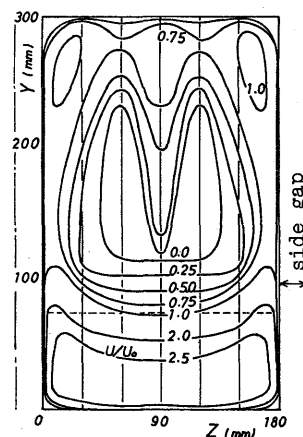


Fig. 9 Velocity diagram of the section ($\beta=40^\circ$, $X/h=1.63$, $2t/B=0.21$).

flow. But in the range of $\beta < 40^\circ$ the characteristics of jet flow is much different and the jet width is large but the core region is very small (Fig. 7). This suggests that the velocity reduction in jet flow is mainly due to the interaction between the momentum of jet and the wall friction, and that a jet with high velocity but small mass flow volume is decelerated rapidly to the downstream.

As for the velocity recovery in the separation zone, the side-gap leakage has large influence. When the side-gap is narrowed, the recovery of the separation zone becomes much smaller as shown by the dotted line in Fig. 6(a) and even a reverse flow appears. In order to study the velocity recovery in the separation zone, the longitudinal (Y-directional) and lateral (Z-directional) velocity distributions of the section at $X/h=1.63$ are shown in Fig. 8. In the range of $Y/h < 0.124$, corresponding to the core width of the jet, there is seen a good two-dimensional flow field in Fig. 8(a), but in the other range the velocity variation is large in the lateral direction. Especially in the range of $Y/h > 0.4$ the velocity peaks are seen both in the central region and near the side walls. To show this clearer, the equi-velocity diagram is shown in Fig. 9 at $X/h=1.63$. In the separation zone at the back of the plate the side-gap-leakage flows diagonally upward from both side gaps to the duct upper wall, is turned to the center and then rolled up to the inner region forming a pair of vortices. Accordingly the side-gap leakage supplies momentum to the separated zone from both sides, the upper side and the center, which makes the recovery of the separation zone very rapid.

After all it is concluded that the side-gap-leakage accelerates the velocity recovery in the separation zone, though the existence of the potential core in the jet region decelerates the velocity reduction in jet. Accordingly, in the case of a large side-gap and a small valve opening angle the plate outlet flow becomes uniform very soon.

Figure 10 shows comparison of the present theory with the measurements at $X/h=1.63$ as for the velocity ratio of the

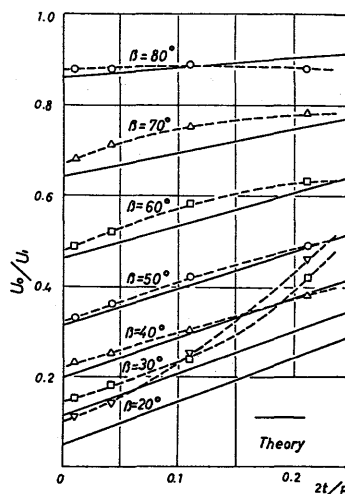


Fig. 10 Influence of side-gap ratio on the velocity ratio of jet.

jet U_1 to the upstream one U_0 and the influence of the valve opening angle and the side-gap ratio $2t/B$. It is seen that the leakage effects can be well predicted by the present theory except for the case of small valve opening angle and large side gap. As the jet width varies little for the variation of side gap as shown in Fig. 7, it is possible to estimate leakage volume from Fig. 8. That is, the ratio of $(U_1/U_0)_{t=0} - (U_1/U_0)_{t=0}$ to $(U_1/U_0)_{t=0}$ gives the ratio of the leakage volume to the mainflow volume. Then it follows that the leakage volume in the case $\beta=80^\circ$ is nearly zero even for a large side gap and in the case $40^\circ < \beta < 70^\circ$ the leakage increases almost linearly with the side gap. In the case $\beta < 30^\circ$ the leakage increases remarkably with an increase in the side gap and the rate of increase becomes especially large when the side gap becomes larger than a value at which the leakage volume amounts to the same as the main flow one. In such cases the present theory gives much smaller value to the measured data, as the velocity profile of the jet flow is sharp with no core region and the reduction of the jet velocity becomes rapid due to wall friction.

Though the velocity variation of the plate outlet flow is very large in Y-direction, the static pressure in the section is almost uniform as shown in Fig.11 except just after the plate exit. The static pressure is also largely influenced by the side-gap, as it changes the jet velocity largely.

Figure 12 shows the wall pressure variation along a duct wall. In the upstream of the valve chamber the pressure is almost uniform along a duct wall, but at the valve plate it drops remarkably and recovers a little just behind the plate. And then it drops and recovers again at the exit of the valve chamber due to the contraction of the channel width and it becomes almost constant at $X'/L' > 0.6$. In a separated flow it is usual that the pressure of a separation zone recovers gradually toward the downstream direction due to velocity reduction in the main flow, but in this type of flow the influence of side-gap-leakage is so large that the recovery of the separation zone is very rapid as already described and a uniform flow is formed soon behind the valve plate. For a comparison, the pressure variation in the case of small side-gap($t=1\text{mm}$) is also illustrated by a dotted line in Fig.12, which shows typical pressure recovery in the separated flow.

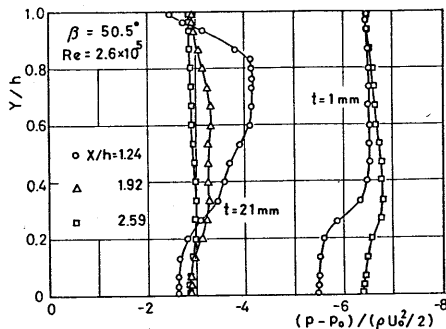


Fig. 11 Static pressure distribution in the section behind the valve plate. ($Z/B' = 0.5$)

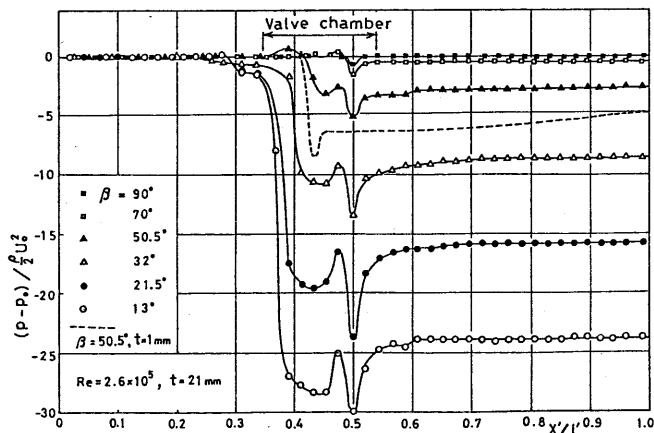


Fig. 12 Static pressure variation along the side wall ($Y/h=0.5$).

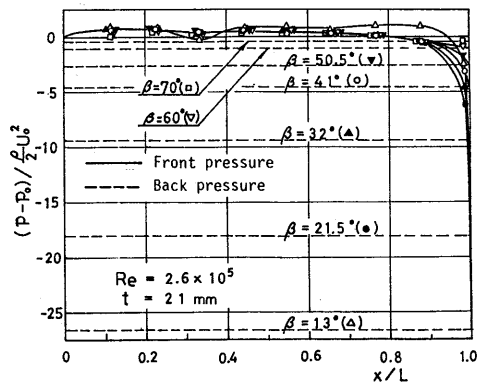
3.2 Pressure distribution on the valve plate and fluid force

Pressure distribution along the centerline of the valve plate is shown in Fig. 13 in the mainstream direction ($Z/B = 0.5$) and the transverse one ($x/L=0.5$) together with the plate back pressure P_B for the case of large side gap ($2t/B=0.21$). It is recognized that the pressure on the plate is almost uniform and is nearly equal to the upstream pressure P_0 for any plate angle β . In the region near the tip and on both sides of the plate it drops sharply to a back pressure but its range is very narrow. It is then suggested that the fluid force acting on the plate might be well estimated by approximating a constant pressure over the plate surface, that is $P=P_0$. When the plate angle is large, such treatment is not adequate, but the fluid force becomes so small that no problem arises in the practical application.

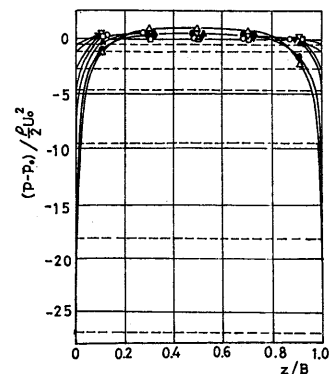
However, in the case of a small side gap the pressure drop at the plate tip becomes very large as shown in Fig.14 for $\beta=40^\circ$. Even in this case the variation of pressure in the transverse direction is still small as shown in Fig.14(b).

One of the important factors of the valve plate is a coefficient of plate back pressure which represents a pressure drop at the valve plate and is defined as

$$C_{pB} = (P_0 - P_B) / (\rho U_0^2 / 2) \dots\dots\dots(4)$$

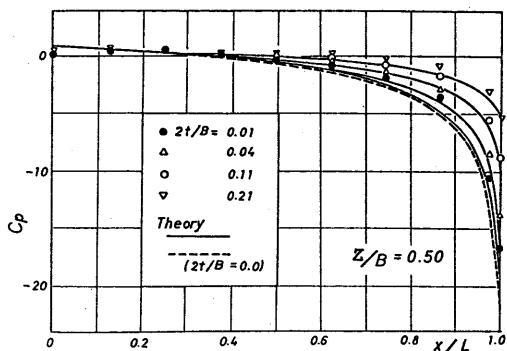


(a) Mainstream direction ($Z/B=0.5$).

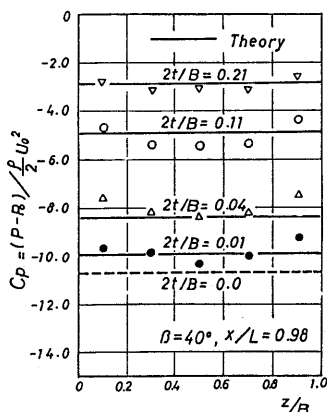


(b) Lateral direction ($x/L=0.5$).

Fig. 13 Static pressure distribution on the valve plate.



(a) Mainstream direction(Z/B=0.5).



(b) Lateral direction(x/L=0.98)

Fig. 14 Influence of side gap on the pressure distribution of valve plate. ($\beta = 40^\circ$)

Figure 15 shows the variation of C_{PB} for the variation of a plate angle β and the side-gap-leakage effects. In the range of $\beta > 60^\circ$ the back pressure varies little for the variation of the side-gap, but for $\beta < 40^\circ$ it drops remarkably with a decrease in β and $2t/B$. For example, in the case of $\beta = 20^\circ$ the back pressure increases eight times when the side gap is narrowed from 21 mm to 1 mm.

The back pressure is essentially dependent upon the jet velocity even if there exists large side-gap-leakage, and therefore it is to be expressed as a function of only the velocity ratio U_0/U_1 of the upstream to the downstream. Figure 16 shows the relation between C_{PB} and U_0/U_1 , from which it is confirmed that almost all the measured data fall on one curve for any side-gap ratio with a few exceptions of the case of $\beta = 20^\circ$.

In Figs.14, 15 and 16 the present theory gives good results and predicts the side-gap-leakage effects with good accuracy, which shows that the pressure at the front and the back surfaces of the valve plate is mainly dependent upon the jet velocity and is little influenced by the strongly three-dimensional flow at the back of the plate in the range that the leakage volume is less than the mainflow one.

The fluid force F acting on the valve plate is obtained by integrating the pressure distribution over the plate. Figure 17 shows the dependence of a normal force coefficient defined as follows upon β .

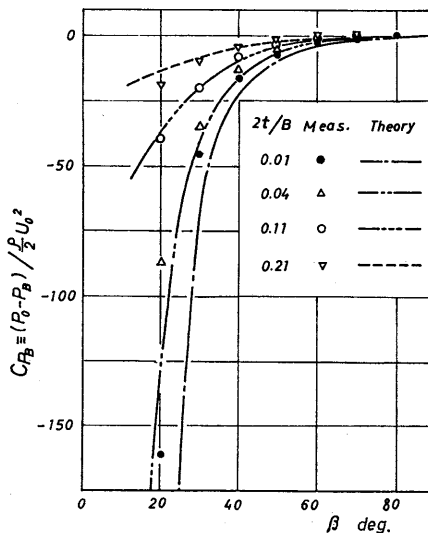


Fig. 15 Back pressure coefficient vs. valve opening angle β and side-gap-leakage effects.

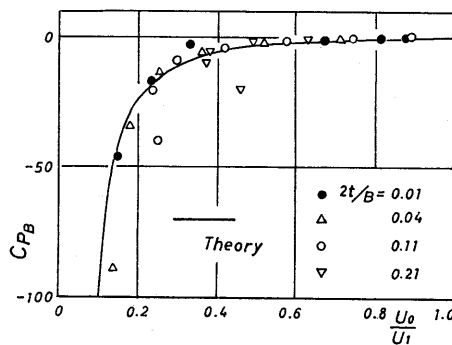


Fig. 16 Back pressure coefficient vs. velocity ratio U_0/U_1 of jet.

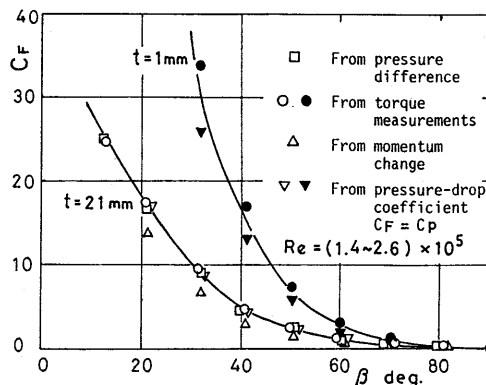
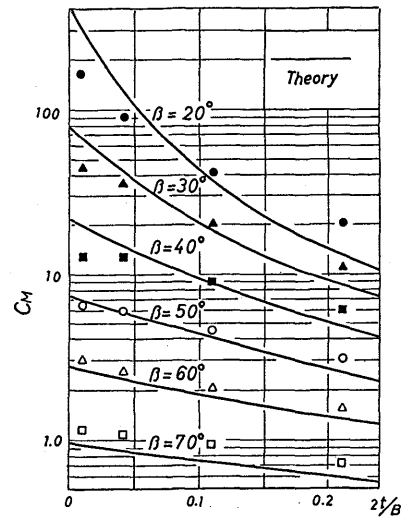
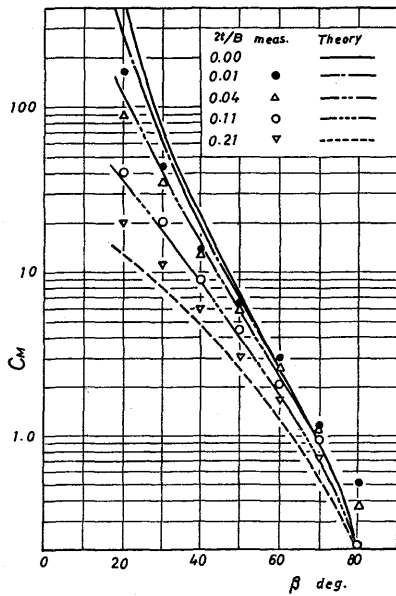


Fig. 17 Normal force coefficient and comparison of several different measurements.

$$C_F = F / (\rho U_0^2 B L / 2) \dots \dots \dots (5)$$

For comparison, the C_F -value is obtained by several different methods, that is the integrated value from the pressure distribution, the measured moment data around the plate axis divided by the radius $L/2$ of the plate gravity centre, the momentum change between the upstream and the downstream and also the approximated value



(a) As a function of valve opening angle β . (b) As a function of side-gap ratio $2t/B$.
 Fig. 18 Variation of moment coefficient C_M and comparison with the present theory.

$C_F = C_p$ obtained by putting $P = P_o$ over the whole plate as described before.

In the case of a large side gap ($t = 21\text{mm}$ or $2t/B = 0.21$) the C_F values obtained by various methods agree well with one another, which shows that the rough approximation of $P = P_o$ over the whole plate for any plate angle β is a reasonable approximation in calculating the fluid force. And also the fact that the C_F value obtained from the momentum change is less than that by the other method indicates that the side-gap-leakage takes out large momentum to the separation zone.

The fluid force acting on a plate induces a moment M around the plate axis and the moment coefficient defined as follows is one of the important factors of a swing-type check valve.

$$C_M = M / (\rho U_o^2 L^2 B / 4) \dots\dots\dots (6)$$

Figure 18 shows the dependence of C_M on β and $2t/B$ and compares the theory with the measurements. Figure 19 also shows the C_M value vs. the velocity ratio U_o/U_1 of the jet, in which the data are expected to fall on one curve for any valve opening angle β and side-gap ratio $2t/B$.

As the back pressure drops remarkably with a decrease in β as already shown in Fig. 15, the moment coefficient C_M increases remarkably with a decrease in β . For example, when the valve opening angle is decreased from 80° to 20° the C_M value increases as much as $200 \sim 400$ times. Moreover, the smaller the plate angle is, the larger the influence of side-gap-leakage becomes, and accordingly the C_M value changes remarkably for the variation of the side-gap when the plate angle is small. For example, a decrease in the side-gap ratio from 0.21 to 0.01 in the case of $\beta = 20^\circ$ results in an increase in the C_M value to as much as 10 times.

From these figures the present theory is seen to predict the side-gap-leakage ef-

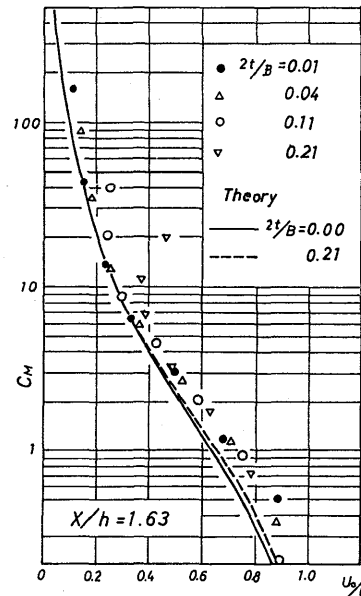


Fig. 19 Moment coefficient as a function of velocity ratio of jet.

fects with good accuracy. However, from a viewpoint of the practical application it will be convenient to estimate the C_M value by a simple equation. From the measured data the following empirical formula is obtained.

$$C_M = 10^{(70-\beta)(0.0412-0.07t/B)} (\beta \text{ deg.}) \dots (7)$$

For the range of $\beta > 70^\circ$ the accuracy of this formula becomes lower but considering that such a large valve opening is not usual in a swing-type check valve, the above formula is useful in estimating C_M value roughly.

From Fig. 19 it is also seen that the C_M value is expressed as a function of only U_o/U_1 for any β and $2t/B$ values.

5. Conclusions

Flow characteristics around a swing type valve plate installed in a rectangular duct are studied theoretically and experimentally. The conclusions are summarized as follows.

- (1) Three dimensional side-gap-leakage effects and fluid force acting on a valve plate can be well predicted by a small modification of the conventional two-dimensional potential flow theory.
- (2) Just behind the valve plate is formed a separation zone, but the side-gap-leakage is rolled up to the centre and forms a vortex pair at the centre of the separation zone and supplies momentum from every side, which makes recovery of the separation zone rapid. In the case of a large side-gap the velocity recovery is very rapid and a uniform flow is formed soon behind the valve plate. But in the case of a small side-gap the recovery is very slow and a core region in the jet flow is maintained to the downstream, which delays the reduction of jet velocity, and the pressure is gradually recovered in the downstream.
- (3) The pressure coefficient on the front and the back surfaces of the plate and the moment coefficient are determined only by the velocity ratio of the jet to the upstream flow for any valve opening angle and side-gap ratio, when the side-gap-leakage volume is less than the main flow volume.
- (4) The outlet flow at the exit of the valve plate is not contracted with the

width nearly equal to the valve opening one, which is similar to the characteristics of nozzle outlet flow.

(5) When the side gap is large, the pressure on the front surface of the plate becomes nearly uniform for any plate opening angle and is equal to the upstream one. This leads to a simple approximation $C_{p_F} = C_{p_M}$ in predicting the fluid force of a valve plate.

(6) For the convenience of practical application an empirical formula is presented for the moment coefficient of the valve plate.

Acknowledgement

The authors would like to express their gratitude to Prof. R. Ooba, Tohoku University, for the valuable suggestions, to Dr. M. Ooshima and Mr. S. Saito, Ebara Co. Ltd., for the experimental apparatus, and to Mr. J. Kawana and Mr H. Sakamoto for the assistance in experiments.

References

- (1) Kurokawa, J., Uchida, T. and Kusa, T., Bulletin of the JSME, Vol.29, No.250 (1986), p.1129.
- (2) Kane, R. S. and Cho, S. M., Proc. Am. Soc. Civ. Eng., HYI(1976), p.57.
- (3) Yamamoto, K. and Nakamura, H., Turbomachinery(in Japanese), Vol.9, No.10 (1981), p.579.
- (4) Birkhoff, G. and others, Q. Appl. Math., Vol.8, No.2(1950), p.151.